Table 9.4 The rise in the watertable at x = 25 m shown at 5-day intervals from the beginning of the rise in the canal stage

Time after t = 0 (d)	u (-)	E_4 (-)	$s_{0,t}$ (m)	$s_{25,t}$ (m)
1	1.25	0.0224	0.04	0.00
5	0.56	0.2353	0.20	0.05
10	0.40	0.3699	0.40	0.15
15	0.32	0.4583	0.60	0.28
20	0.28	0.5085	0.80	0.41
25	0.25	0.5492	1.00	0.55

where

$$E_3(u) = E_2(u) - u\sqrt{\pi}\,E_1(u)$$

Values for the functions $E_3(u)$ and $E_4(u)$ are given in Table 9.1, as well as by Huisman (1972). Equation 9.43 gives the discharge for one side of the canal. If the drop in the canal stage induces groundwater flow from two sides, the discharge given by Equation 9.43 must be multiplied by two.
The solution is also valid for a linearly rising canal stage.

Example 9.5
Suppose that in the situation described in Example 9.3 the canal stage had not risen suddenly at t = 0, but has risen as a function of time, reaching a rise of 1 m after 25 days. Calculate the rise in the watertable at a point x = 25 m from the canal after 1, 5, 10, 15, 20, and 25 days. Also calculate the seepage from one side of the canal per metre length on the 5th day.

For s_o = 1 m and t = 25 days, the proportionality factor α in Equation 9.41 is

$$\alpha = \frac{1}{25} = 0.04$$

For the distance x = 25 m and the given times t for which the watertable rise is to be calculated, the value of u is computed with Equation 9.35. For each value of u, the corresponding value of $E_4(u)$ is read from Table 9.1. The water level in the canal at time t is found from Equation 9.41, with the proportionality factor α = 0.04. Substituting this value and the value of $E_4(u)$ into Equation 9.42 gives the rise in the watertable (Table 9.4).

9.6 Periodic Water-Level Fluctuations

9.6.1 Harmonic Motion

In some instances, the variations in the level of bodies of surface water are periodic. Examples are the twice-daily variation in the level of oceans, seas, and coastal rivers due to the tide.

The rise and fall of the sea level induces corresponding variations in groundwater pressure in underlying or adjacent aquifers. If the sea level varies with a simple harmonic motion, which is usually expressed as a sine or cosine function, a sequence of sinusoidal waves is propagated inland from the submarine outcrop of the aquifer. Water levels in observation wells placed in the aquifer at different distances from the coastline or river bank will therefore show a similar sinusoidal motion. However:

- The amplitude of the sinusoides decreases with the distance from the sea or river; in other words, the waves are damped inland;
- The time lag (phase shift) of a given maximum or minimum water level increases inland.

It is clear that there must be a relationship between the damping and the phase shift on the one hand and the aquifer characteristics on the other. An analysis of the propagation of tidal waves through an aquifer allows these characteristics to be determined. The only data required are water-level records from some observation wells placed at various distances in a line perpendicular to the coast or river. The records must cover at least half a cycle so that phase shift and damping can be determined. Preferably, several full cycles should be recorded and their average values used, because the damping and phase shift may be different for the maximum and the minimum of the curve.

The harmonic motion of the sea level (Figure 9.10) can be described by

$$y_o = \bar{y} + A \sin \omega t$$

where

y_o = water level with respect to a certain reference level (m)
$\bar{y}$ = mean height of the water level with respect to the same reference level (m)
A = amplitude of the tidal wave, i.e. half range of the sea level change (m)
$\omega = 2\pi/T$ = wave frequency (d^{-1})
T = period required for a full cycle (d)
t = time elapsed from a convenient reference point within any cycle (d)

The analysis of tidal waves will be discussed in Chapter 24.

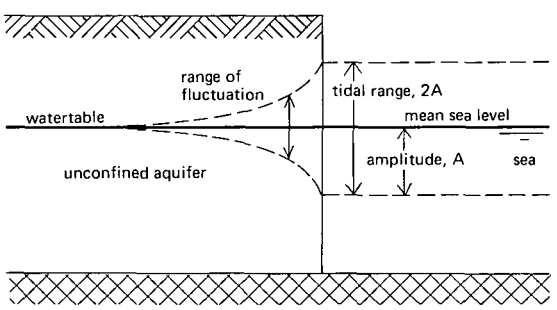

Figure 9.10 Watertable fluctuations induced by ocean tides

Assuming that the storage of water through compression effects in the aquifer is negligible, Steggewentz (1933) derived the following equation for the hydraulic head in an aquifer at a distance x from the coast or tidal river, and at a time t

$$h(x,t) = \bar{h} + A\, e^{-ax} \sin(\omega t - bx) \tag{9.46}$$

where

$h(x,t)$ = hydraulic head in the aquifer at distance x and at time t (m)
$\bar{h}$ = mean hydraulic head in the aquifer at distance x (m)
bx = phase shift, expressed in radians (–)
e^{-ax} = amplitude reduction factor (–)

Both damping and phase shift depend on the distance x from the open water (x = 0 at the boundary of land and water).

Differentiating Equation 9.46 with respect to x and t, and substituting the result into the differential equation describing the groundwater flow, yields the relation between the constants a and b, and the aquifer characteristics, as shown in the following sections.

9.6.2 Tidal Wave Transmission in Unconfined Aquifers

Steggewentz (1933) found for the relation between a, b, and the aquifer characteristics of an unconfined aquifer that

$$a = b = \sqrt{\frac{\mu\omega}{2KD}} \tag{9.47}$$

where

a = amplitude damping coefficient (m^{-1})
b = phase shift coefficient (m^{-1})
μ = specific yield of the aquifer (–)
KD = transmissivity of the aquifer (m^2/d)
ω = frequency of the tidal wave (d^{-1})

Note that in an unconfined aquifer the damping and the phase shift are the same. If this is not so, the aquifer is semi-confined.

9.6.3 Tidal Wave Transmission in a Semi-Confined Aquifer

When considering the propagation of a tidal wave through confined or semi-confined aquifers, we must take into account the compressibility of the water and the solid medium. In doing so, Jacob (1940, 1950) derived expressions for the propagation of tidal fluctuations through a completely confined aquifer. Bosch (1951) extended Jacob's theory to semi-confined aquifers by including the effect of leakage through the confining layer covering the aquifer. The situation is similar to that shown in Figure 9.1 except that the water level in the river, y_o, fluctuates periodically with a range

2A. (The half range or amplitude of the tidal wave is thus A). The differential equation that describes this flow problem reads as follows

$$\frac{\partial^2 h}{\partial x^2} - \frac{h - h'}{KDc} - \frac{S}{KD}\frac{\partial h}{\partial t} = 0 \qquad (9.48)$$

where

h = the hydraulic head in the aquifer (m)
h′ = the watertable elevation in the confining layer (which is assumed to remain constant) (m)
S = the storativity of the aquifer (–)
x = the distance from the river, measured along a line perpendicular to the river (m)
t = time (d)

All other symbols are as defined earlier.

The storativity of a saturated confined aquifer was defined in Chapter 2.3.1. In unconfined aquifers, the storativity, S, is considered equal to the specific yield, μ, because the effects of aquifer compression and water expansion are generally negligible.

A decrease in hydraulic head infers a decrease in hydraulic or water pressure, p_h, and an increase in intergranular pressure, p_i (see Chapter 13.3). If h decreases, the water released from storage is produced by two mechanisms:
– The compression of the aquifer caused by increasing p_i;
– The expansion of the water caused by decreasing p_h.

The first of these mechanisms is controlled by the compressibility of the aquifer, α, and the second by the compressibility of the water, β. This leads to the concept of specific storage

$$S_s = \rho g(\alpha + \varepsilon\beta) \qquad (9.49)$$

where

S_s = specific storage (m^{-1})
α = compressibility of the aquifer (Pa^{-1})
β = compressibility of the water (Pa^{-1})
ρ = density of water (kg/m^3)
g = acceleration due to gravity (m/s^2)
ε = porosity of the aquifer material (–)

The storativity of the aquifer is then defined as

$$S = S_s D \qquad (9.50)$$

which, when substituted into Equation 9.49, becomes

$$S = \rho g D(\alpha + \varepsilon\beta) \qquad (9.51)$$

Since the compressibility is the inverse of the modulus of elasticity, Equation 9.51 may also be written as

$$S = \rho g D \left(\frac{1}{E_a} + \frac{\varepsilon}{E_w} \right) \tag{9.52}$$

where

E_a = modulus of elasticity of the aquifer material (Pa)
E_w = modulus of elasticity of water (Pa)

The compressibility α of sand is in the range of 10^{-7} to 10^{-9} Pa^{-1}, and the compressibility of water, β, can be taken as 4.4×10^{-10} Pa^{-1}.

The solution of Equation 9.48 is

$$h(x,t) = h' + A\, e^{-ax} \sin(\omega t - bx) \tag{9.53}$$

Differentiating with respect to x and t and substituting the result into Equation 9.48 yields

$$(a^2 - b^2) \sin(\omega t - bx) + 2ab \cos(\omega t - bx) - \frac{1}{KDc} \sin(\omega t - bx)$$

$$- \frac{\omega S}{KD} \cos(\omega t - bx) = 0 \tag{9.54}$$

For this equation to be valid for all values of x and t, the constants a and b must satisfy the following conditions

$$a^2 - b^2 = \frac{1}{KDc} \tag{9.55}$$

$$2ab = \frac{\omega S}{KD} \tag{9.56}$$

These relations indicate that if the constants a and b can be determined from field observations, the hydraulic characteristics KDc and S/KD can be calculated.

Example 9.6

The horizontal propagation of tidal fluctuations emanating from the River Waal in The Netherlands has been measured in an adjacent semi-confined aquifer. The 34 m thick aquifer consists of coarse sands with intercalations of fine sand. The aquifer is overlain by a 12 m thick confining layer of clayey fine sands and heavy basin clays, with intercalations of peat. It is underlain by a layer of heavy clay, which is assumed to be impermeable.

Figure 9.11 shows the hydrographs of some of the piezometers that were placed in the aquifer along a line perpendicular to the river.

From these hydrographs, we read the amplitude A and, by comparing the hydrographs of the piezometers with the hydrograph of the river, we can determine the time lag of each piezometer. To express the phase shift in radians, we multiply the time lag t by $2\pi/T$.

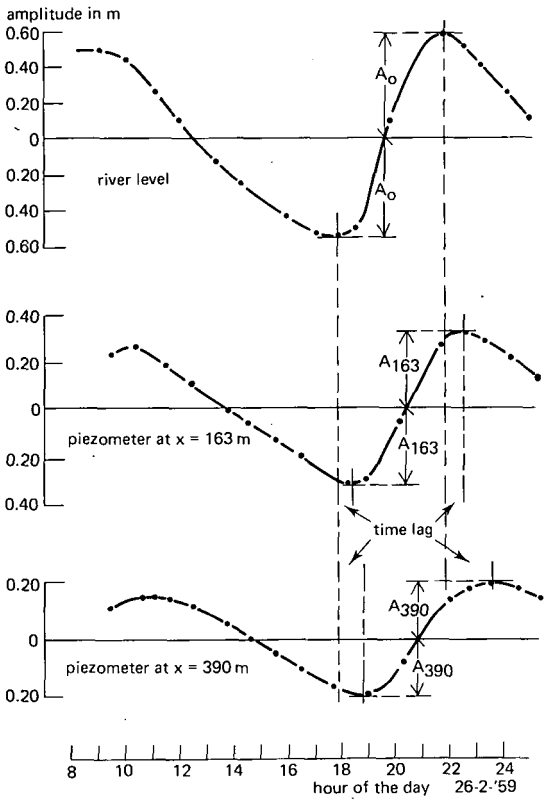

Figure 9.11 Hydrographs of the River Waal and of two piezometers at 163 and 390 m from the river (after Wesseling and Colenbrander 1962)

Note that the time lag after low tide is less than that after high tide. The average time lag and the average amplitude are therefore used in the calculations.

From Equation 9.53, it is clear that the amplitude A_o at $x = 0$ and the amplitude A_x at any arbitrary value of x are related as follows

$$A_x = A_o e^{-ax}$$

In other words, the amplitude ratio is

$$\frac{A_x}{A_o} = e^{-ax}$$

or

$$\ln \frac{A_x}{A_o} = -ax \tag{9.59}$$

This expression indicates that, when plotting the natural logarithm of the amplitude ratio as a function of the distance x to the river, we find a straight line whose slope, a, can be determined. Theoretically, this line should pass through the origin, since at $x = 0$, $A_x = A_o$, and $\ln A_x/A_o = \ln 1 = 0$. In practice, this hardly ever happens

because of the entry resistance at the river. A thin resisting layer may be present at the outcrop, or the river may only partially penetrate the aquifer.

When we plot the phase shift (in radians) against the distance x to the river, we obtain a straight line whose slope b can be determined. Figure 9.12 shows these plots of the amplitude ratios and phase shifts for three piezometers at different distances from the river.

From Figure 9.12, we find that the slope of the amplitude ratio line

$$a = \frac{1}{430} = 2.3 \times 10^{-3}$$

and the slope of the phase shift line

$$b = \frac{0.9}{600} = 1.5 \times 10^{-3}$$

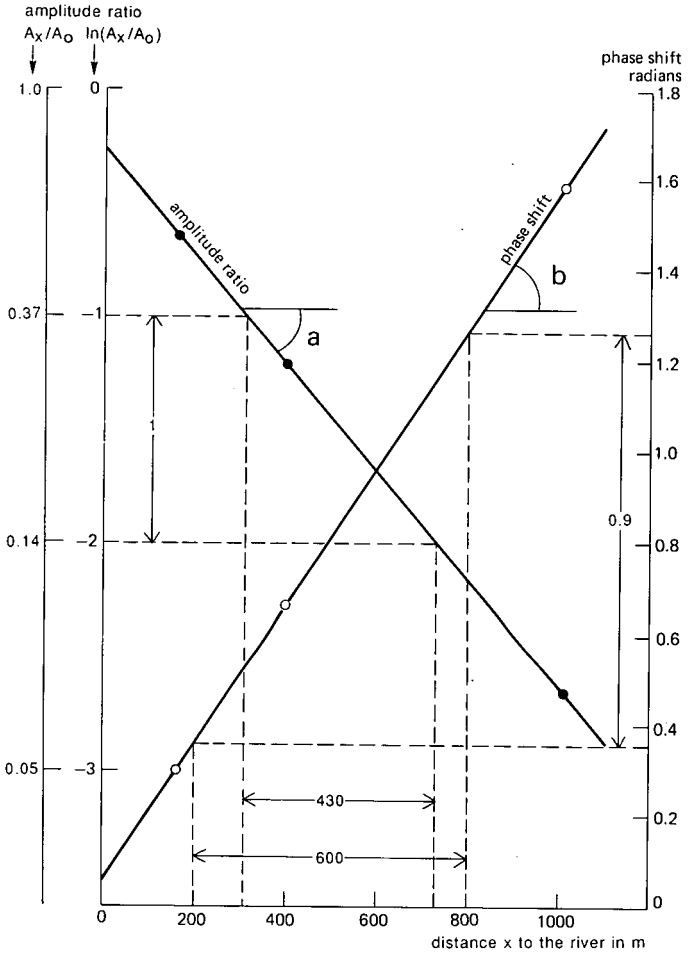

Figure 9.12 Relation between amplitude ratio and phase shift, and the distance of three piezometers placed in a row perpendicular to the River Waal (after Wesseling and Colenbrander 1962)

With a and b known, we can now calculate the leakage factor $L = \sqrt{KDc}$, using Equation 9.55

$$\frac{1}{KDc} = a^2 - b^2 = (2.3 \times 10^{-3})^2 - (1.5 \times 10^{-3})^2 = 3.04 \times 10^{-6}$$

$$KDc = 328\,947\ m^2$$

$$L = \sqrt{328947} = 574\ m$$

From Equation 9.56 we find

$$\frac{S}{KD} = \frac{2ab}{\omega} = \frac{2 \times 2.3 \times 10^{-3} \times 1.5 \times 10^{-3}}{2 \times (3.14/0.5)} = 5.5 \times 10^{-7}\ d/m^2$$

Remarks
For accurate determinations of the maximum and minimum water levels in the sea, in a tidal river, and in piezometers, frequent observations must be made at high and low tide. Accurate hydrographs (as shown in Figure 9.11) can be obtained with automatic water-level recorders. If, for some reason, water-level measurements cannot be made in the sea or tidal river, the data from the piezometer nearest to the sea or river can be used as a reference for calculating the amplitude ratios and phase shifts of the piezometers farther inland.

9.7 Seepage from Open Channels

In irrigation areas, the water level in the canals is, in general, higher than the watertable of the adjacent land. Owing to this head difference, seepage occurs from the canals to the adjacent land. Analytical solutions for steady-state seepage from open channels have been developed by a number of investigators. For instance, Vedernikov (1934) gave solutions to the problem of seepage from trapezoidal channels to drainage layers at finite and infinite depths. Dachler (1936) presented a solution for the seepage from a canal embedded in uniform soil with a shallow watertable, consequently causing the watertable to merge with the water level in the canal. Kozeny (1931) treated the seepage from canals with a curvilinear cross section in infinitely deep soil without a watertable.

Bouwer (1965, 1969) studied the seepage from open channels, using electric resistance network analogs. Bouwer's approach covers a wider range of soil conditions, depths and shapes of the channel, and watertable positions than the earlier studies. He also presented graphs that are more readily applicable. We shall therefore review part of his work. For more details, we refer the reader to Bouwer's papers cited above.

9.7.1 Theoretical Models

Seepage from channels is a dynamic process that is complicated by a variety of factors: e.g. non-uniformity of soil, water quality, erosion, sedimentation, soil permeability, fluctuating watertables and water levels in the canals, and periodic filling and drying

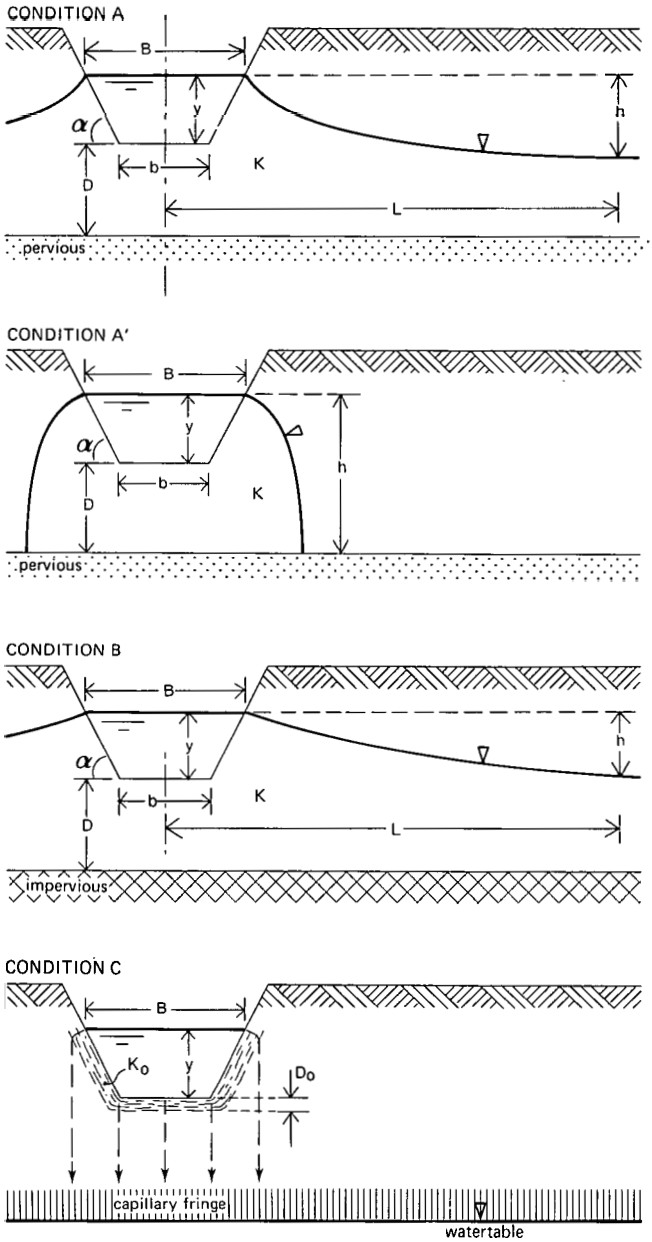

Figure 9.13 Geometry and symbols for Seepage Conditions A, A′, B, and C (after Bouwer 1965, 1969)

up of the canals. To obtain solutions to seepage problems, Bouwer recognized that simplifications of the actual field situations must be introduced. Accordingly, he distinguished the following basic seepage models (Figure 9.13).

Condition A: The soil in which the channel is embedded is uniform and is underlain

by a layer that is more permeable than the overlying soil. (That layer is considered infinitely permeable.) If the watertable is at or below the top of the permeable underlying layer, Condition A reduces to the case of seepage to a free-draining layer, where $h = y + D$. This will be referred to as Condition A′.

Condition B: The soil in which the channel is embedded is uniform and is underlain by a layer that is less permeable than the overlying soil. (That layer is considered impermeable.)

Condition C: The soil in which the channel is embedded is much less permeable than the original soil, because sedimentation has formed a thin layer of low permeability at the channel perimeter (clogged soil, compacted soil linings).

9.7.2 Analog Solutions

Bouwer's studies of canal seepage with a resistance network analog included analyses of Conditions A, A′, and B. The solutions he found apply to steady-state conditions. In reality, however, canal seepage is seldom steady because of changing water levels in the canal, changing watertables, etc. Thus, the steady-state conditions covered by the analyses represent individual pictures of a system which, in reality, tends to be continuously unsteady.

Mathematically, the above seepage problems are treated with lateral boundaries at infinity. In reality, this is impractical because physical barriers, e.g. other canals or streams, may be present. Finite lateral boundaries should be used instead.

For Condition A: The slope of the watertable decreases as the distance from the canal increases, and reaches zero at infinity. For practical purposes, the slope of the watertable can be considered zero at a finite distance from the canal. Bouwer used an arbitrary distance $L = 10b$, from the centre of the canal. The head at this point is h. The watertable is considered a solid boundary, i.e. it is assumed that the movement of the watertable over the distance 10b is sufficiently small for flow components normal to the watertable to be insignificant.

For Condition A, the lower limit of the watertable is at the top of the permeable layer, where $h = y + D$, and Condition A′ is reached. Even if the watertable were to be below the top of the permeable layer, the pressure at the top of this layer would still be zero (atmospheric).

For Condition B: As the flow approaches uniform flow, the slope of the watertable at a sufficient distance from the canal becomes essentially constant. Thus the lateral boundary for the flow system can be represented by a vertical equipotential, which Bouwer also took at a distance of 10b from the centre of the canal. From test results, he found that this distance was sufficiently long for the establishment of an essentially horizontal watertable for Condition A, and a watertable with essentially constant slope for Condition B. The practical implications are that at $L = 10b$ the direct effect of the seepage on the watertable is insignificant, and that the position of the watertable at that point can be regarded as indicative of the 'original' watertable position controlling the flow system adjacent to the canal.

For practical purposes, the underlying layer can be treated as infinitely permeable (Condition A) if its hydraulic conductivity, K, is ten times greater than that of the overlying layer. The underlying layer can be treated as impermeable (Condition B) if its hydraulic conductivity, K, is ten times less than that of the overlying material. In the analog studies, the values of y, h, and D were varied. The seepage for the condition of an infinitely deep, uniform soil ($D = \infty$) was evaluated by extrapolating D to infinity for the analysis of Condition A.

The analog analyses were performed for trapezoidal canals with a 1:1 side slope ($\alpha = 45°$) and three different water depths (expressed as y/b).

The seepage rates, measured as electric current, were converted to volume rate of seepage, q_s, per unit length of canal. These rates were divided by the water-surface width of the canal, B, to yield the rate of fall, I_s, of the water surface due to seepage, as if the canal were ponded. The term I_s is expressed per unit hydraulic conductivity of the soil, K, in which the canal is embedded to yield the dimensionless parameter, I_s/K. To yield dimensionless terms, all length dimensions are expressed as ratios to the bottom width b of the canal.

Figure 9.14 shows the graphs of I_s/K-versus-h/b for different values of D/b for three different water depths, expressed as y/b.

Example 9.7

Calculate the seepage from a trapezoidal canal embedded in a soil whose hydraulic conductivity K = 0.5 m/d. The soil layer is underlain by a highly permeable layer at 8 m below the bottom of the canal. The water depth in the canal is 1 m, the bottom width of the canal is 2 m, and the surface water width is 4 m. The watertable at 20 m

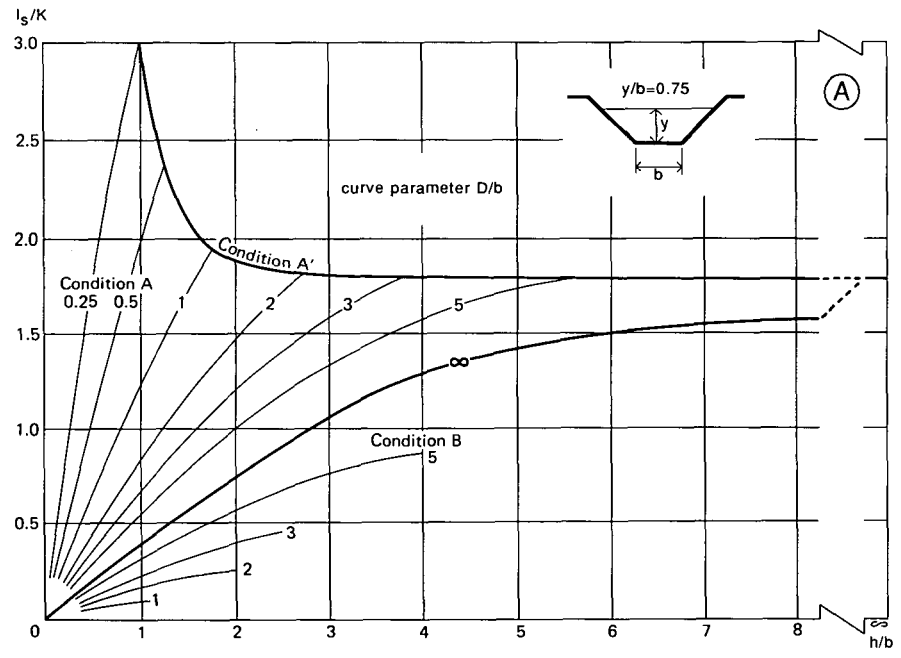

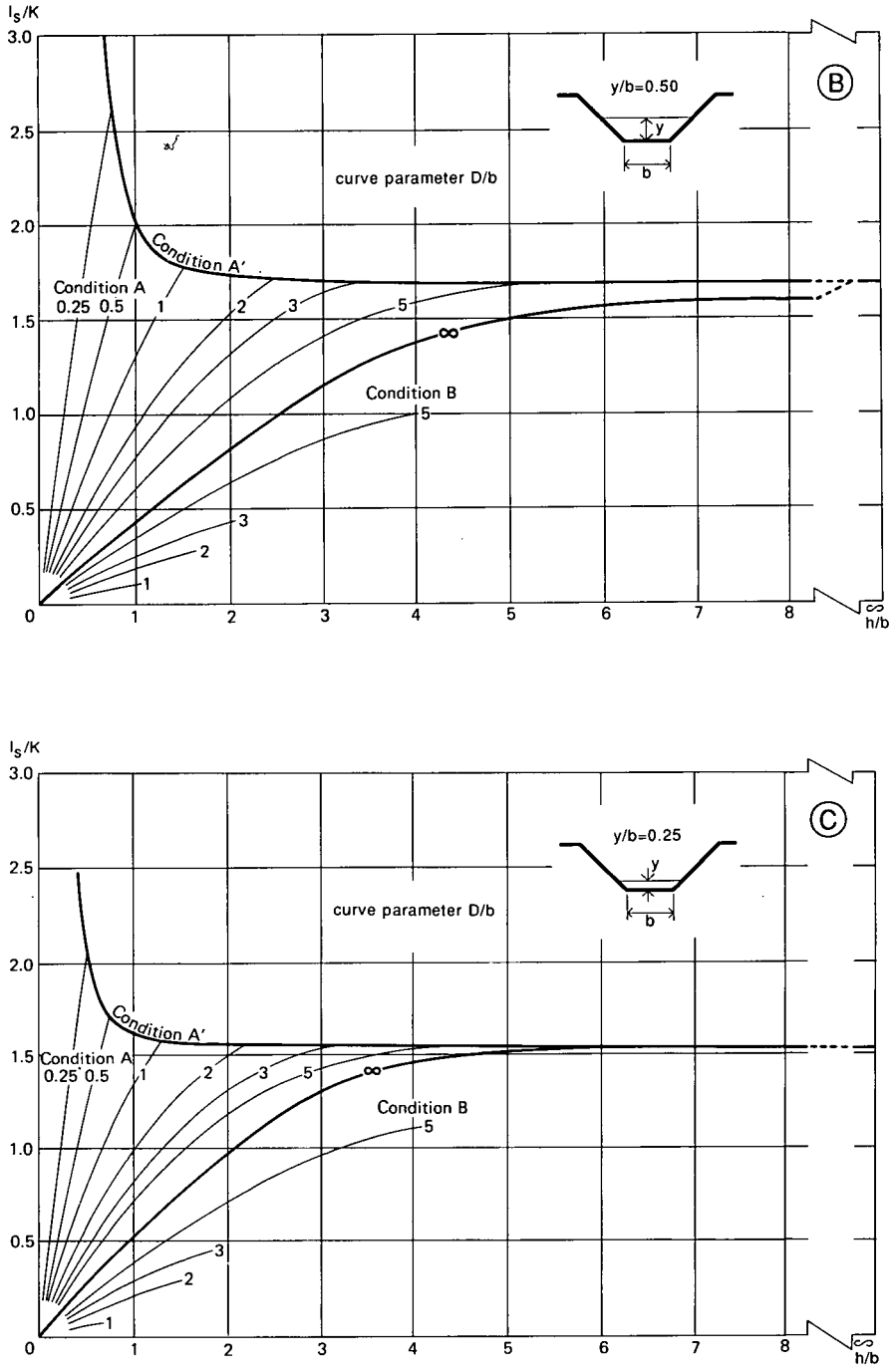

Figure 9.14 Results of seepage analyses with electric analogs for trapezoidal canal with 1:1 side slopes ($\alpha = 45°$) at three different canal stages (after Bouwer 1965, 1969)
A: $y/b = 0.75$; B: $y/b = 0.50$; C: $y/b = 0.25$

from the canal is 5 m below the water surface in the canal. Thus: h = 5 m, y = 1 m, b = 2 m, D = 8 m and B = 4 m.
Hence, h/b = 5/2 = 2.5, and D/b = 8/2 = 4. Since y/b = 0.5, we use Figure 9.14B and find that I_s/K = 1.4, which, for K = 0.5 m/d, and B = 4 m, gives a seepage loss per metre length of canal:

$$q_s = 1.4 \times 0.5 \times 4 = 2.8 \text{ m}^2/\text{d}$$

Figure 9.15 shows examples of flow systems (streamlines and equipotential lines) for Conditions A, A′, and B, as obtained by electric analog analyses.

The curves for Condition A′ in Figure 9.14 are the loci of the end points of the curves for Condition A. At these points, h = D + y, and any further lowering of the watertable will not increase the effective value of h. Thus, for Condition A′, the h/b-values at the abscissa should be interpreted as (D + y)/b.

The curves for Condition A in Figure 9.14 indicate that the effect that a permeable layer at depth has on seepage becomes rather small if that layer is deeper than five times the bottom width of the canal (D > 5b). High values of I_s/K are obtained for relatively small values of D, particularly if h approaches D + y.

For Condition A′, the graphs show that the seepage rate remains almost constant at a wide range of depths of the permeable layer (effective head h = D + y). If this depth becomes less than three times the water depth in the canal (D < 3y), the seepage increases rapidly.

For Condition B, we can make similar observations on the position of the impermeable layer. The graphs show that, for a given watertable position, the seepage

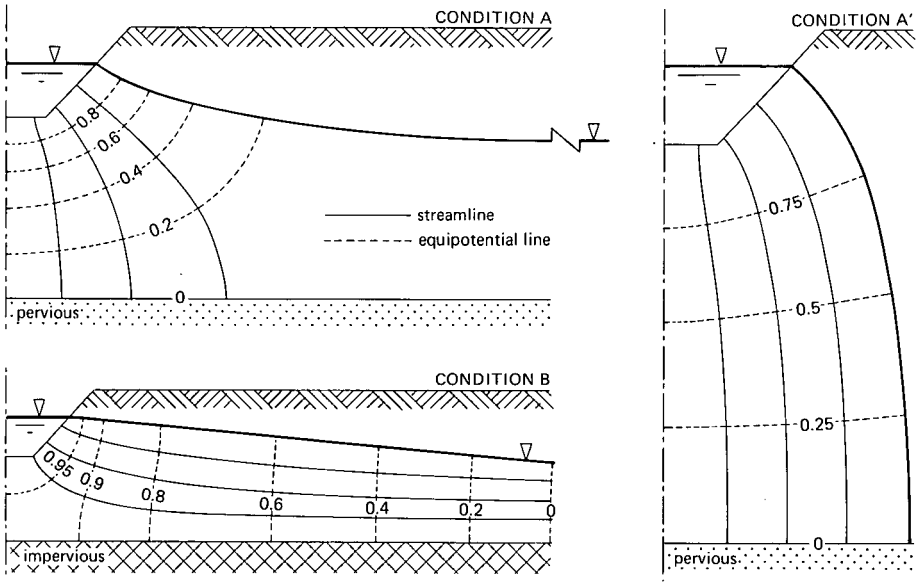

Figure 9.15 Flow systems for seepage under different conditions, obtained by electric analog analysis; equipotentials expressed as fraction of total head (after Bouwer 1965, 1969)

initially increases linearly as the depth of the impermeable layer (D) increases, but that the rate of increase diminishes as D becomes relatively large. For $D > 5b$, I_s/K is already relatively close to the values for $D = \infty$. Obviously, an impermeable layer only has a significant effect on seepage if its depth below the canal bottom is less than five times the bottom width of the canal. As we have seen above, the same applies to a permeable layer. A practical implication of these findings is that exploratory borings to determine the potential seepage from new irrigation canals need not penetrate deeper than approximately 5b below the projected elevation of the canal bottom.

The effect of the watertable on seepage shows a similar trend. Consider, for instance, the curve for $D = \infty$. Initially, the seepage (I_s/K) increases almost linearly with h, but for relatively large values of h the increase of the seepage diminishes. If h has reached a value of approximately three times the width of the water surface in the canal ($h = 3B$), the value of I_s/K is already close to that of $h = \infty$. Thus, a general lowering of the watertable, e.g. by pumping from wells, would result in a significant increase in seepage only if the initial depth of the watertable were considerably less than 3B below the water surface in the canal.

To apply the graphs of Figure 9.14 to canals of other shapes, we can compute b from the actual values of B and y, as if the canal were trapezoidal with $\alpha = 45^0$, or we can replace the cross-section with the best-fitting trapezoidal cross-section with $\alpha = 45^0$. For water depths other than those of Figure 9.14, values of I_s/K can be evaluated by interpolation.

9.7.3 Canals with a Resistance Layer at Their Perimeters

Some canals have a relatively thin layer of low permeability along their wetted perimeter (Condition C, Figure 9.13). Such a resistance layer may be natural in origin (e.g. sedimentation of clay and silt particles and/or organic matter, or biological action), or artificial (e.g. earthen linings for seepage control).

If the hydraulic conductivity of the resistance layer (K_o) is sufficiently small to cause the rate of downward flow in the underlying soil to be less than the hydraulic conductivity K of this soil, then the soil beneath the resistance layer will be unsaturated (provided that the watertable is sufficiently deep for the canal bottom to be well above the capillary fringe, and that air has access to the underlying soil). Under these conditions, the flow beneath the resistance layer will be due to gravity alone – and thus at unit hydraulic gradient – and the (negative) soil-water pressure head, h_1, in the zone between the resistance layer and the top of the capillary fringe will be uniform. The infiltration rate, i, at any point of the canal bottom can therefore be described with Darcy's equation as

$$i = K_o \frac{y + D_o - h_1}{D_o} \tag{9.60}$$

where

i = infiltration rate (m/d)
K_o = hydraulic conductivity of the resistance layer (m/d)

D_o = thickness of the resistance layer (m)
y = depth of the water above the resistance layer (m)
h_1 = soil-water pressure head (m)

This equation can be simplified if we consider that resistance layers are usually thin (clogged surfaces, sediment layers), so that D_o will be small compared with $y - h_1$ and can be neglected in the numerator. If the thickness of the resistance layer is small, it may be difficult to determine the actual value of D_o. The same is true for K_o. Under these circumstances, the hydraulic property of the resistance layer is more conveniently expressed in terms of its hydraulic resistance, C_o, defined as D_o/K_o (dimension: time). Equation 9.60 then reduces to

$$i = \frac{y - h_1}{C_o} \tag{9.61}$$

Applying this equation to the seepage through the bottom and the sides of a trapezoidal canal, and assuming that C_o is uniform and that the flow through the layer on the canal sides is perpendicular to the bank, we obtain the following equation for the seepage q_s

$$\begin{aligned} q_s = I_s B &= (i_{\text{bottom}} \times b) + \left(i_{\text{side slope}} \times \frac{2y}{\sin\alpha}\right) \\ &= \frac{y - h_1}{C_o} b + \frac{\frac{1}{2}y - h_1}{C_o} \times \frac{2y}{\sin\alpha} \\ &= \frac{1}{C_o}\left[(y - h_1) b + (y - 2h_1)\frac{y}{\sin\alpha}\right] \end{aligned} \tag{9.62}$$

References

Abramowitz, M. and I.A. Stegun 1965. Handbook of mathematical functions: with formulas graphs and mathematical tables. Dover, New York, 1045 p.

Bear, J., D. Zaslavsky and S. Irmay 1968. Physical principles of water percolation and seepage. Arid Zone Research 29 UNESCO, Paris, 465 p.

Bosch, H. 1951. Geohydrologisch onderzoek Bergambacht (unpublished research report).

Bouwer, H. 1965. Theoretical aspects of seepage from open channels. Journal of the Hydraulics Division, 91, pp. 37-59.

Bouwer, H. 1969. Theory of seepage from open channels. In: V.T. Chow (ed.). Advances in Hydroscience, 5, Academic Press, New York. pp. 121-172.

Bouwer, H. 1978. Groundwater hydrology. McGraw-Hill, New York, 480 p.

Colenbrander, H.J. 1962. Een berekening van hydrologische bodemconstanten, uitgaande van een stationaire grondwaterstroming. In: De waterbehoefte van de Tielerwaard-West, Wageningen. 135 p.

Dachler, R. 1936. Grundwasserströmung. Springer, Wien.

Dwight, H.B. 1971. Tables of integrals and other mathematical data. 4th ed. MacMillan, New York, 336 p.

Edelman, J.H. 1947. Over de berekening van grondwaterstromingen. Thesis, Delft University of Technology (Mimeographed).

Edelman, J.H. 1972. Groundwater hydraulics of extensive aquifers. ILRI Bulletin 13, Wageningen, 216 pp.

Ferris, J.G., D.B. Knowles, R.H. Brown and R.W. Stallman 1962. Theory of aquifer tests. U.S. Geological Survey Water Supply Paper 1536-E, Washington, pp. 69-174.

Harr, M.W. 1962. Groundwater and seepage. McGraw-Hill, New York, 315 p.

Huisman, L. 1972. Groundwater recovery. Macmillan, London, 336 p.

Jacob, C.E. 1940. On the flow of water in an elastic artesian aquifer. Transactions American Geophysical Union, 2, pp. 574-586.
Jacob, C.E. 1950. Flow of groundwater. In: H. Rouse (ed.). Engineering hydraulics, Wiley, New York. pp. 321-386.
Jahnke, E. and F. Emde 1945. Tables of functions with formulae and curves. 4th ed. Dover, New York, 304 p.
Kozeny, J. 1931. Grundwasserbewegung bei freiem Spiegel, Fluss und Kanalversickerung. Wasserkraft und Wasserwirtschaft, 26, 3 p.
Muskat, M. 1946. The flow of homogeneous fluids through porous media. McGraw-Hill, New York, 763 p.
Rushton, K.R. and S.C. Redshaw 1979. Seepage and groundwater flow: numerical analysis by analog and digital methods. Wiley, New York, 339 p.
Steggewentz, J.H. 1933. De invloed van de getijbeweging van zeeën en getijrivieren op de stijghoogte van het grondwater. Thesis, Delft Univiversity of Technology, 138 p.
Vedernikov, V.V. 1934. Versickerungen aus Kanälen. Wasserkraft und Wasserwirtschaft, 11-13, 82 p.
Verruijt, A. 1982. Theory of groundwater flow, 2nd ed., MacMillan, London, 144 p.
Wesseling, J. and H.J. Colenbrander 1962. De bepaling van hydrologische bodemconstanten uit de voortplanting van de getijbeweging. In: De waterbehoefte van de Tielerwaard-West, Wageningen. 135 p.